

Entrance Channel Dependent Light Charged Particle Emission from the ^{156}Er Compound Nucleus

J. F. Liang, J. D. Bierman,* M. P. Kelly, A. A. Sonzogni, R. Vandenbosch, and J. P. S. van Schagen

Nuclear Physics Laboratory, Box 354290, University of Washington, Seattle, Washington 98195

(Received 11 June 1996; revised manuscript received 22 November 1996)

Light charged particle decay from the ^{156}Er compound nucleus, populated by $^{12}\text{C}+^{144}\text{Sm}$ and $^{60}\text{Ni}+^{96}\text{Zr}$ at the same excitation energy, were measured in coincidence with the evaporation residues. The high energy slope of charged particle spectra for the ^{60}Ni -induced reaction is steeper than for the ^{12}C -induced reaction. Model calculations including particle evaporation during fusion result in good agreement with the data. This suggests that the difference in the charged particle spectra between the two entrance channels is due to a longer formation time in the ^{60}Ni -induced reaction. [S0031-9007(97)02930-X]

PACS numbers: 25.70.Gh, 21.65.+f, 24.60.Dr, 25.70.Jj

The time scale for large scale rearrangement of nuclear matter is one of the important problems in nuclear physics. It is influenced by the mechanism of nuclear dissipation which can be probed in nuclear fission and fusion reactions [1]. Several experiments have been performed at excitation energies near 53–56 MeV to look for possible entrance channel effects in fusion reactions. When a compound nucleus is populated from entrance channels with significantly different formation times, one may be able to observe different behaviors in the decay of the compound nucleus. Mixed results were obtained. For instance, the spectrum of the high energy γ rays from the decay of the giant dipole resonance built on excited states in ^{164}Yb formed by $^{64}\text{Ni}+^{100}\text{Mo}$ did not agree with statistical model calculations. Nevertheless, no disagreement was observed in the same compound nucleus formed in the $^{16}\text{O}+^{148}\text{Sm}$ reaction [2]. In a later study differences were observed in the charged particle multiplicity ratios d/p and α/p for the two reactions which were attributed to the longer shape equilibration time in the mass more symmetric channel [3]. Another well studied case was the ^{156}Er compound nucleus which was populated by two different entrance channels, $^{12}\text{C}+^{144}\text{Sm}$ and $^{64}\text{Ni}+^{92}\text{Zr}$. The neutron multiplicities measured from the mass nearly symmetric entrance channel failed to meet the expectation from a statistical model, whereas for the $^{12}\text{C}+^{144}\text{Sm}$ reaction the experimental data and model calculations are in good agreement [4]. However, the results of light charged particle and γ -ray measurements were inconclusive [5].

It is assumed that a compound nucleus has no memory of its formation. In a statistical model, for a given excitation energy and angular momentum, the compound nucleus decay should be independent of the entrance channel [6]. Dynamical effects were introduced to explain the entrance channel dependence of the ^{164}Yb data. It is known that nuclear dissipation will prolong the fusion process, in particular for the mass symmetric entrance channels [7]. If the compound nucleus formation time is longer than the evaporative lifetime of the dinuclear system, particle

and γ -ray emission may take place before the system reaches equilibrium, thus reducing the excitation energy of the compound nucleus. In Ref. [2], the γ -ray spectrum was reproduced by calculations taking into account particle evaporation and γ -ray emission during the formation stage.

In this Letter, the study of light charged particles emitted from the ^{156}Er compound nucleus populated by two entrance channels is presented. The aim of the present experiment was to clarify the situation by going to higher excitation energies where the nuclear evaporation times, which serve as a clock, are an order of magnitude faster. In order to make comparisons between the two reactions, it is important to match the excitation energy and angular momentum. The angular momentum distributions for the two entrance channels can be matched if for both systems the largest angular momentum contributing to fusion is larger than the critical angular momentum l_c^{ER} , above which no evaporation residues (ERs) survive fission competition. In laboratory experiments, this can be achieved by measuring coincidences between the decay particles and ERs from a compound nucleus.

The experiments were carried out in the Nuclear Physics Laboratory at the University of Washington. The compound nucleus ^{156}Er was populated by $^{12}\text{C}+^{144}\text{Sm}$ and $^{60}\text{Ni}+^{96}\text{Zr}$ at an average excitation energy of 113 MeV. The fission barriers at the maximum angular momentum of the reaction fall below the neutron binding energy. This gives a similar spin distribution for fusion leading to ERs for both systems. At such a high excitation energy, charged particle decay competes more effectively with neutron and γ -ray emission. Beams of ^{12}C , $E_{\text{lab}} = 142$ MeV, and ^{60}Ni , $E_{\text{lab}} = 333$ MeV were produced by the tandem-linac accelerator and were incident on isotopically enriched ^{144}Sm ($200 \mu\text{g}/\text{cm}^2$ on a $15 \mu\text{g}/\text{cm}^2$ carbon foil) and ^{96}Zr ($1 \text{mg}/\text{cm}^2$, self-supporting) targets, respectively. Angular distributions of light charged particles were measured by three CsI scintillators, coupled to PIN diode detectors, in coincidence with ERs. Light charged particles were identified by pulse

shape discrimination techniques. The CsI-PIN diode detectors were calibrated by elastic scattering of protons and α particles. The linearity in energy response of the CsI crystal over the region of interest is excellent. ERs were separated from the beam by a pair of electrostatic deflectors and collected by a large area ($6 \times 4 \text{ cm}^2$) silicon strip detector placed downstream, 82 cm from the target. The identification of ERs was obtained by their time of flight and energy using the linac RF clock as a reference.

The energy spectra of light charged particles were transformed to the center of mass frame of the compound nucleus. For the same reaction, the spectral shape is nearly identical for center of mass angles greater than 85° . Figure 1 shows the particle spectra for protons and α particles in the center of mass frame. The dynamic range of the data extends over three decades. Only statistical uncertainties are presented in the figure. As can be seen, the light charged particles emitted from the ^{60}Ni -induced reaction are softer than those from the ^{12}C -induced reaction. The multiplicity ratios of the two reactions as a function of particle energy, shown on the right panels of the figure, further demonstrate the difference in the slope. This suggests that for the ^{60}Ni -induced reaction the particles were emitted from a colder source.

To examine if there were kinematic biases in the data, the experimental apparatus was simulated in Monte Carlo calculations taking events from statistical model calculations. The charge state distribution of the ERs, the multiple scattering of ERs in the target, the size of

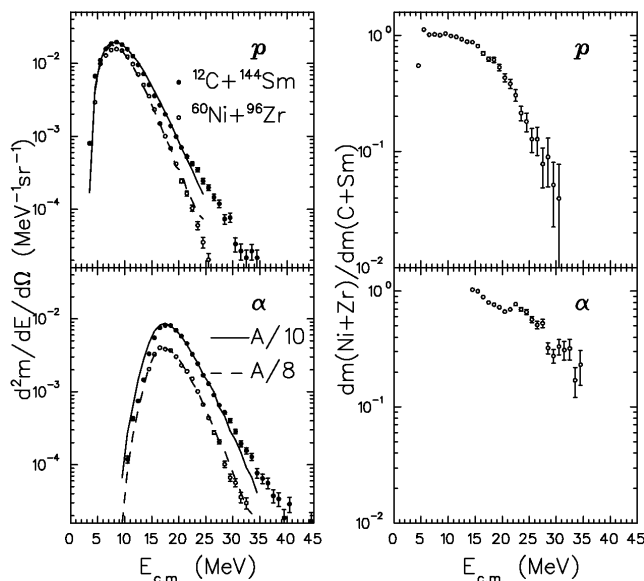


FIG. 1. Left panels: Light charged particle energy spectra for $^{12}\text{C} + ^{144}\text{Sm}$ and $^{60}\text{Ni} + ^{96}\text{Zr}$ at $\theta_{\text{lab}} = 130^\circ$ and $\theta_{\text{lab}} = 80^\circ$, respectively. The proton spectra are shown in the upper panel and the α -particle spectra are in the lower panel. The results of statistical model calculations are shown by the solid curves ($a = A/10$) and the dashed curves ($a = A/8$), and are normalized to the data. Right panels: Multiplicity ratios for the two reactions as a function of particle energy after normalizing to the multiplicities at the peaks of the spectra.

the beam, and the angular acceptance of the detector were taken into account. In the simulations, the efficiencies as a function of particle energy for all the detector angles were calculated. For a given deflector angle the efficiency corrections differ with LCP detection angle, as the optimum deflector angle depends on the LCP detection angle. We present here data for LCP detectors where the deflector position was optimum. The comparisons of the raw data and the efficiency corrected particle spectra are shown in Fig. 2. As can be seen, the efficiency corrected particle spectra at these angles are very similar to the raw data. This shows that the slope differences in the high energy particle spectra cannot be the result of kinematic biases. We find the kinematic biases do have an observable effect on the angle-integrated multiplicities, in particular for α particles, but not on the spectral shape. This Letter will emphasize comparisons of the spectral shape. The absolute multiplicities will be discussed in a longer paper.

Since the projectile energy for the $^{12}\text{C} + ^{144}\text{Sm}$ reaction is greater than 10 MeV per nucleon, it is necessary to consider preequilibrium emission which is characterized by particle spectra with a very shallow slope and energies extending to several times the projectile energy per nucleon. Possible evidence for such a contribution can be seen in the proton spectrum of Fig. 1. A Fermi

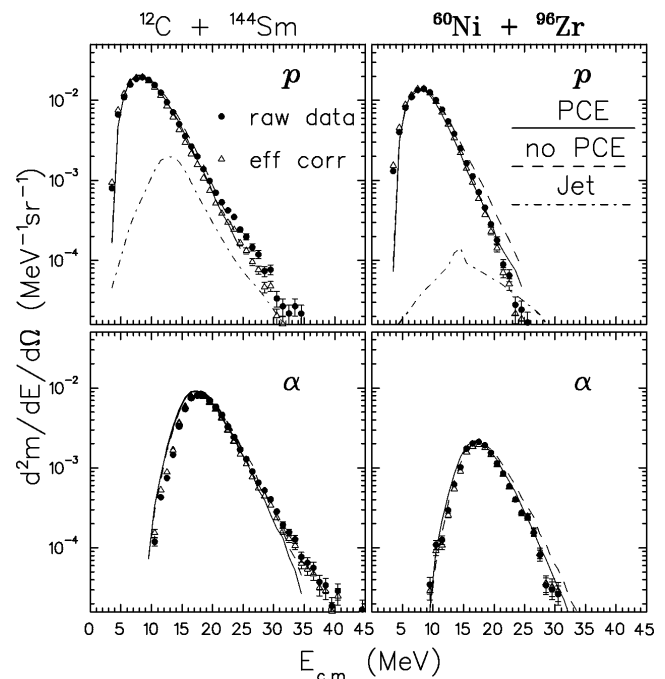


FIG. 2. Upper panels: Proton spectra for $^{12}\text{C} + ^{144}\text{Sm}$ ($\theta_{\text{lab}} = 130^\circ$) and $^{60}\text{Ni} + ^{96}\text{Zr}$ ($\theta_{\text{lab}} = 80^\circ$). The raw data (\bullet) and Monte Carlo corrected data (Δ) are presented. The dashed curve is for statistical model calculations without PCE. The solid curve is the result of calculations considering particle evaporation during formation. The contribution of preequilibrium jet particles is shown by the dash-dotted curves and included in the dashed and solid curves. Lower panels: α -particle spectra for $^{12}\text{C} + ^{144}\text{Sm}$ and $^{60}\text{Ni} + ^{96}\text{Zr}$.

jet model [7] was used to estimate the contribution of preequilibrium emission. This estimate is rather uncertain at the very low bombarding energies employed in the present study as the model was developed for and is applicable at several tens of MeV per nucleon. The diffuseness of the Fermi momentum distribution was adjusted in the calculation to reproduce the highest energy part of the $^{12}\text{C}+^{144}\text{Sm}$ data, as shown by the dash-dotted curves in Fig. 2. This calculation overestimates the contribution for $^{60}\text{Ni}+^{96}\text{Zr}$ and should be considered as an upper limit only. When this component was subtracted from the proton spectra, the differences in the high energy slopes for the two different entrance channels still persist. The Fermi jet mechanism is not appropriate for modeling complex particles like α particles. α particles from breakup of ^{12}C would be strongly forward peaked, whereas at the backward angles the spectral shape does not depend on angle.

Before pursuing the causes for the differences in the particle spectra, comparison between the data and statistical model calculations using the Monte Carlo code EVAP [9] assuming all particle evaporation follows compound nucleus formation is presented. In order to be assured that the spin window up to l_c^{ER} was being filled the ER cross section for $^{60}\text{Ni}+^{96}\text{Zr}$ was extrapolated from Ref. [10]. The ER cross section for $^{12}\text{C}+^{144}\text{Sm}$ was measured in a separate experiment which will be reported elsewhere. The l_c^{ER} extracted from the ER cross sections was $l_c^{\text{ER}} = 57\hbar$, which agrees with an estimate by the rotating liquid drop model [11]. The calculated ER cross sections using the Sierk fission barrier [12] and $a_f/a = 1.07$ agree with the experimental measurements. As shown by the solid curves in Fig. 1, a level density parameter of $a = A/10$ was used to reproduce the high energy slope of the preequilibrium emission corrected data for the $^{12}\text{C}+^{144}\text{Sm}$ reaction while as shown by the dashed curves $a = A/8$ was needed for the $^{60}\text{Ni}+^{96}\text{Zr}$ reaction. This difference in the level density is not expected for a compound nucleus of the same excitation energy and angular momentum distributions. Some theoretical models show that for mass $A \approx 150$ at excitation energies near 100 MeV the level density parameter is $a = A/10$ [13]. In order to reproduce the peak energy of the particle spectra, an emitter deformation was introduced to lower the Coulomb barrier for charged particle emission [14]. Transmission coefficients and the yrast line were calculated assuming a prolate shape emitter. Good agreement with the data was achieved by a deformation parameter $\beta_2 = 0.25$, as shown in Fig. 1.

Since the corrections discussed above cannot account for the slope difference between the two reactions, the possibility of differences in the formation leading to the different spectra is examined. A one-body dissipation code HICOL [7] was used to estimate the amalgamation time. The amalgamation times were determined by the time required to reach a shape whose quadrupole moment has fallen to that of a prolate deformed ellipsoid with an axis ratio of 1.3. This assures a shape that is more com-

pact than that of the unconditional saddle. The amalgamation times for the ^{60}Ni -induced reaction are two to four times longer than those of the ^{12}C -induced reactions, as shown in the top panel of Fig. 3. The excitation energy as a function of time is plotted at the mean spin, $l \approx 40\hbar$, of the reaction in the bottom panel. Although somewhat faster for the lighter projectile system $^{12}\text{C}+^{144}\text{Sm}$, energy dissipation occurs rather rapidly compared to shape equilibrium. For the $^{60}\text{Ni}+^{96}\text{Zr}$ system the shape equilibration time, $\sim 50 \times 10^{-22}$ s, is significantly longer than the 20×10^{-22} s calculated evaporative lifetime of the composite system. Therefore, particle evaporation during this period should be considered. It should be noted that these evaporated particles are to be distinguished from those emitted by the Fermi jet mechanism mentioned above as the preequilibrium emission. They will be called the precompound evaporation or evaporation during formation below. A simplified model which uses a statistical theory to account for particle evaporation during the formation period was devised. In the present model, the formation time was divided into several time intervals comparable to or less than the length of the lifetime as shown in Fig. 3. The lifetime of the composite system in a time interval was calculated using the average excitation energy and the average shape, given by HICOL, of that time

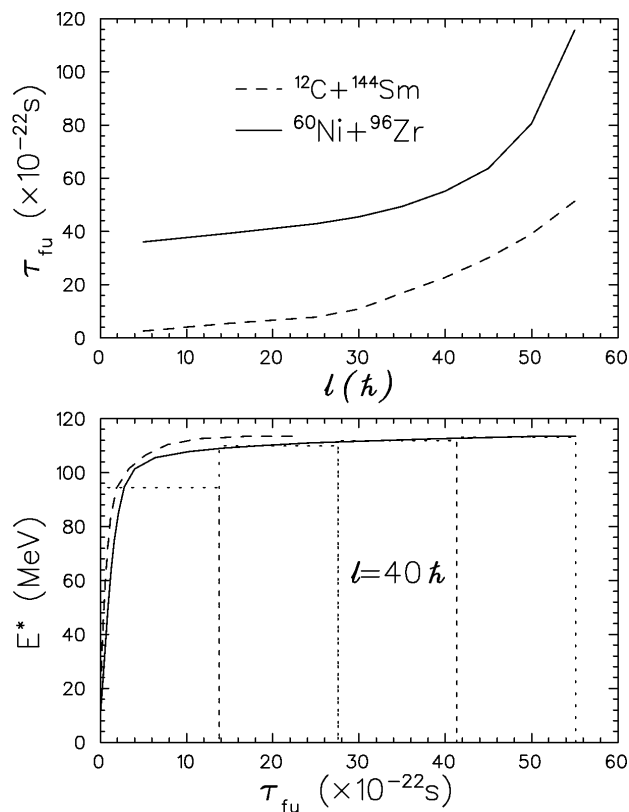


FIG. 3. Top panel: Amalgamation time as a function of angular momentum. Bottom panel: Excitation energy as a function of amalgamation time for $l = 40\hbar$. The solid curve is for $^{60}\text{Ni}+^{96}\text{Zr}$, and the dashed curve is for $^{12}\text{C}+^{144}\text{Sm}$. The dotted lines show how the amalgamation period was divided to estimate precompound evaporation.

interval. The probability of the dinuclear system surviving without evaporating a particle follows the decay law $\exp(-\Delta t/\tau)$, where Δt is the duration of a time interval and τ is the particle decay lifetime which is calculated by EVAP. If a particle was evaporated, the excitation energy of the dinuclear system will be reduced accordingly. Since Δt is very short, the possibility of emitting a second particle in the same time interval is negligible. Only one particle evaporation in each time interval was considered. This generated an input distribution, nuclei of different masses and excitation energies, for the next time interval. Following the same procedure, the calculations were performed throughout the formation stage until the system reached amalgamation. It should be remembered that the statistical model parameters for a dinuclear system during formation are not known. Additionally, the system was not in equilibrium. The results from a statistical model can be used as an estimate only. In order to simplify the calculations, several approximations were made. Only secondary emission following neutron evaporation was considered in the calculations, since the dominant evaporation was neutrons and the average excitation energy carried away by a neutron was estimated to be only a few MeV less than that removed by protons and α particles. The level density parameter was chosen to be $a = A/10$ and fixed throughout the calculations. These approximations were made in order to avoid introducing further free parameters.

When the system has amalgamated, a distribution of equilibrated compound nuclei was produced rather than only ^{156}Er . The decay of the equilibrium compound nuclei was calculated for the distribution of the corresponding excitation energy by the statistical model in a standard way. The light charged particle spectra were summed and weighted by the relative population of the compound distribution. Again, transmission coefficients were calculated for a prolate deformed emitter with a deformation parameter $\beta_2 = 0.25$. The results are shown in Fig. 2. The results of calculations taking into account the effect of formation time are shown by solid curves, while those without the effect of formation are shown by dashed curves. The contribution of the preequilibrium jet particles was included in those curves. For $^{12}\text{C}+^{144}\text{Sm}$, very little difference between the calculations can be seen. Either calculation is in good agreement with the data. For $^{60}\text{Ni}+^{96}\text{Zr}$, the data are well described by calculations including precompound evaporation. Without considering the effect of formation, the slope obviously differs from the data. The cooling of the compound nucleus due to particle evaporation during a long formation time can be seen. The nominal excitation energy is 113 MeV for both reactions. With precompound evaporation (PCE) the mean excitation energy for $^{12}\text{C}+^{144}\text{Sm}$ is 103 MeV and for $^{60}\text{Ni}+^{96}\text{Zr}$ is 94 MeV. The results are similar for the α -particle spectra. The inclusion of particle evaporation during formation in the calculations is qualitatively in better agreement with the data for both reactions. For the

^{12}C -induced reactions, calculations with or without PCE gave similar results.

Some discrepancies between the calculations and data can still be seen in the α -particle spectrum of the ^{60}Ni -induced reaction. The amalgamation time for $^{60}\text{Ni}+^{96}\text{Zr}$ as a function of angular momentum predicted by HICOL is linear for $l \leq 30\hbar$. It increases sharply with angular momentum for $l > 30\hbar$. The calculations were performed at the mean spin of the reaction $l = 40\hbar$ only. More particle evaporation is expected at higher angular momentum which corresponds to longer amalgamation times. Moreover, the partial cross section σ_l at higher angular momentum contributes more to the total ER cross section because of the $(2l + 1)$ factor. On the other hand, HICOL might underpredict the amalgamation time [1].

The entrance channel effects, due to a long formation time, observed in this study are fairly moderate. The lifetime of a composite system is estimated to increase by an order of magnitude when the excitation energy decreases from 113 to 56 MeV. It is therefore somewhat surprising that similar effects were observed in some (but not all) experiments performed at excitation energies near 56 MeV.

In summary, different spectral shapes from the ^{156}Er compound nucleus decay were observed for different entrance channels. The proposed explanation for the softness of the particle spectra for $^{60}\text{Ni}+^{96}\text{Zr}$ is that due to a long amalgamation time particle evaporation during formation reduces the equilibrium excitation energy of the compound nucleus. Calculations taking into account the effect of the long formation time given by a one-body dissipation model are in good agreement with the experimental data.

We wish to thank the accelerator staff for providing the beams. We also thank the staff of the electronics shop and machine shop for technical assistance. This work was supported by the U.S. Department of Energy.

*Present address: Physics Department AD-51, Gonzaga University, Spokane, WA 99258-0051.

- [1] M. Thoennessen, Nucl. Phys. **A599**, 1c (1996).
- [2] M. Thoennessen *et al.*, Phys. Rev. Lett. **70**, 4055 (1993).
- [3] M. Korolija *et al.*, Phys. Rev. C **52**, 3074 (1995).
- [4] W. Kühn *et al.*, Phys. Rev. Lett. **51**, 1858 (1983).
- [5] B. Fornal *et al.*, Phys. Rev. C **42**, 1472 (1990).
- [6] N. Bohr, Nature (London) **137**, 344 (1936).
- [7] H. Feldmeier, Rep. Prog. Phys. **50**, 915 (1987).
- [8] S. J. Luke, R. Vandenbosch, and J. Randrup, Phys. Rev. C **48**, 857 (1993).
- [9] N. G. Nicolis, D. G. Sarantites, and J. R. Beene, computer code EVAP (unpublished).
- [10] R. V. F. Janssens *et al.*, Phys. Lett. B **181**, 16 (1986).
- [11] S. Cohen, F. Plasil, and W. J. Swiatecki, Ann. Phys. (N.Y.) **82**, 557 (1974).
- [12] A. J. Sierk, Phys. Rev. C **33**, 2039 (1986).
- [13] S. Shlomo and J. B. Natowitz, Phys. Rev. C **44**, 2878 (1991).
- [14] J. R. Huizenga *et al.*, Phys. Rev. C **40**, 668 (1989).